ESI Preprints **Not Peer-reviewed**

Rock-Logging-Seismic Integrated Carbonate Reservoir Prediction and Inversion of Mala Oil Field, South Sudan

Mr. Deng Daniel Agwang, Msc. Petroleum Geoscience
Lecturer and Researcher, School of Petroleum and Minerals,
University of Juba (UoJ), Juba, South Sudan

Approved: 08 July 2026
Posted: 10 July 2026

Cite As:
Agwang, D.D. (2026). *Rock-Logging-Seismic Integrated Carbonate Reservoir Prediction and Inversion of Mala Oil Field, South Sudan*. ESI Preprints.
https://doi.org/10.19044/esipreprint.7.2026.p74

Abstract

Carbonate reservoirs are globally known to exhibit commercial hydrocarbon reserves and probable underground storage for carbon dioxide and hydrogen; conversely, uncertainty and error analysis are often overlooked in quantitative log interpretation and the estimation of petrophysical parameters due to the complexity and heterogeneity of subsurface formations. Traditional methods often fall short in addressing such structural intricacy, making it challenging to accurately predict the properties of carbonate reservoirs and infer their potential, as this study aims to predict carbonate reservoir properties using existing petrophysical and reservoir modelling data, which were simulated to generate various cross-plots for interpretation. The analysed cross-plots (Figures 3, 4, 5, 6, 8, and 9) indicate the presence of a dolomitized limestone reef carbonate reservoir. In contrast, the illustrations (Figures 3, 5, 7, and 8) highlight coral and algae, chalky, mudstone sediments characterised as kerogen-rich hydrocarbon, dominantly oil-gas prone, filled with brine (Figure 5, 6, 8, 10, 11, 12, 13, and 14). These are dominated by moldic, vuggy, or karstic porosity. The selected reservoirs of Mala oil field exhibit good characteristics: moldic-vuggy to karstic porosity and partially weathered, dolomitized limestone lithofacies, indicative of reef-associated carbonate systems. These properties not only support their classification as high-quality (Figure 7) reefal carbonate reservoirs but also suggest their suitability for future carbon dioxide (CO_2)

and hydrogen underground storage due to their adequate pore space and potential for long-term seal suppression.

Keywords: Neutron-Density porosity, Simulation, Carbonate, Cross-plot

Introduction

Carbonate reservoirs are recognized as major contributors to global proven hydrocarbon reserves. They are widely distributed across North America, Northern Africa, the Middle East, and Central Asia (Tiab & Donaldson, 2012; Howarth & Alves, 2016; Li et al., 2018). In the context of South Sudan, carbonate reservoirs exhibit limited accumulation patterns, complex structural features, and variable reservoir conditions, indicating a gap in studies. In the context of the literature reviewed, main types of carbonate reservoir include organic reefs and biohermal, shallow-marine, grain beaches, dolomites, chalks, fractured, tight micritic and weathered crust carbonates, these reservoirs are typically large in scale and shallow in burial depth, primarily concentrated in the Jurassic, Cretaceous, and Neogene periods. Most are characterized as pore-type carbonate reservoirs (Tiab & Donaldson, 2012), prestack seismic inversion retains the characteristics that the seismic reflection amplitude varies with the offset or incident angle and can provide more sensitive and effective data volume set. Under the constraint of log data, prestack seismic inversion relies on seismic P-wave and S-wave velocity, density (ρ), and other elastic parameters are carried out to obtain high precision elastic parameters that can reflect lateral changes in reservoirs (Reza et al., 2019).

Previously, reservoir prediction can be modelled from acoustic impedance (Zp) to carbonate reservoir properties as well as lithotypes, and fluid content. Moreover, due to parameters limitations, it cannot clearly distinguish between lithotypes and fluid content. Seemingly, the problem can be resolved by adaptation of shear impedance (Zs) to delineate more carbonate reservoir properties. The combination of acoustic impedance, shear impedance, Vp/Vs, Lambda Rho and Mu Rho can delineate the reservoir properties promptly (Prayoga & Winardhi, 2022). To estimate impedance and porosity, at each well location, the well is calibrated to the seismic and wavelet extraction. The variation between the synthetic seismograms and seismic traces poses significant reading in response to sonic and seismic logs (Alvarez & Gebus, 2011).

Prayoga & Winardhi. (2022), who performed simultaneous inversion coupled with response to extract information from seismic data to compute geological problems that cannot be solved by acoustic inversion. The parameter of Vs in simultaneous inversion is able to compute the dualism between porosity in carbonates and shales, in which Zp has limitations, therefore S-wave parameter is crucial to assess between reservoir and non-reservoir rocks, for conceptual reasoning simultaneous inversion is the optimal approach to anticipate acoustic impedance, shear impedance, and rock density simultaneously to characterize reservoir and to minimize error in the seismic processing (Prayoga & Winardhi, 2022). Rock physics represents the link between geological reservoir parameters (e.g. porosity, clay content sorting, lithology, saturation) and seismic properties (e.g. acoustic impedance, Vp/Vs, density, elastic moduli) are required for prestack seismic inversion. Usually, the combination of P-and S-wave velocities is sensitive to reservoir fluid prediction (Asquith et al., 2004). Rock physics models are used to interpret sonic, and seismic velocities and to predict fluid and lithology substitution (Asquith et al., 2004).

Abuhagaza et al. (2021) & Mohammed. (2023) highlighted that, Mala oil field is located within block 5A of Muglad basin of South Sudan and Sudan covering $120{,}000km^2$ extending from $80km\ NW-SE$ to $NNW-SSEE$ with maximum width of $200km$ that has episode of extensional and strike slip structural histories s shown in Figure 1(Pragst et al., 2017). The reservoir rocks are predominantly sandstones deposited in fluvial-channel, lacustrine and deltaic environment settings. High quality reservoirs were deposited in proximal alluvial-fluvial environments, whereas poor quality reservoirs are associated with more distal lacustrine deposits.

Background

Uncertainty and error analysis are often overlooked in quantitative log interpretation and the estimation of petrophysical parameters, which makes it challenging to accurately predict the properties of carbonate reservoirs. However, accounting for these uncertainties is essential for reliable reservoir prediction and inversion analysis (Avseth, 2010). To estimate petrophysical and rock physics parameters from integrated datasets, such as post-drilled reservoir rock samples and prestack seismic data; prestack and simultaneous seismic inversions are commonly used (Prayoga & Winardhi, 2022; Reza et al., 2019). Despite their usefulness, these inversion methods rely on certain assumptions and require specific input parameters, which are often not readily available in geophysical datasets. These limitations pose significant challenges for geoscientists in effectively predicting carbonate reservoir properties as postulated by Avseth. (2010).

Abuhagaza et al. (2021), who suggested that petrophysical, petrography, scanning electron microscopy. X-ray diffraction, both conventional and special core analysis that characterized the lower cretaceous Bentiu and Abu Gabra Formations of the Muglad Basin produce largest hydrocarbon reservoirs in South Kordofan. Subsequently, based on the integrated study, the Abu Gabra-Bentiu sequence comprises four petrographical microfacies, which consist of two reservoir rock types (quartz arenites and quartz wackes). The reservoir quality is good to excellent porosity (average $\emptyset = 26.7\%$), permeability (average $k = 1365 mD$), Reservoir Quality Index (RQI, average $= 1.43 \mu m$), Flow Zone Indicator (FZI, average $= 3.66 \mu m$) and Discrete Rock Type (DRT, average$= 13$). The relatively low to fair reservoir quality of the Abu Gabra Formation (average $\emptyset = 13.2\%,$ average $k = 14.7 mD,$ average RQI$= 0.17 \mu m,$ average FZI$= 1.05 \mu m, and$ average DRT$= 10$) is due to authigenic kaolinite and siderite content, compaction and cementation by silica and clay patches. This also correlate with similar study as documented (El Sawy et al., 2020).

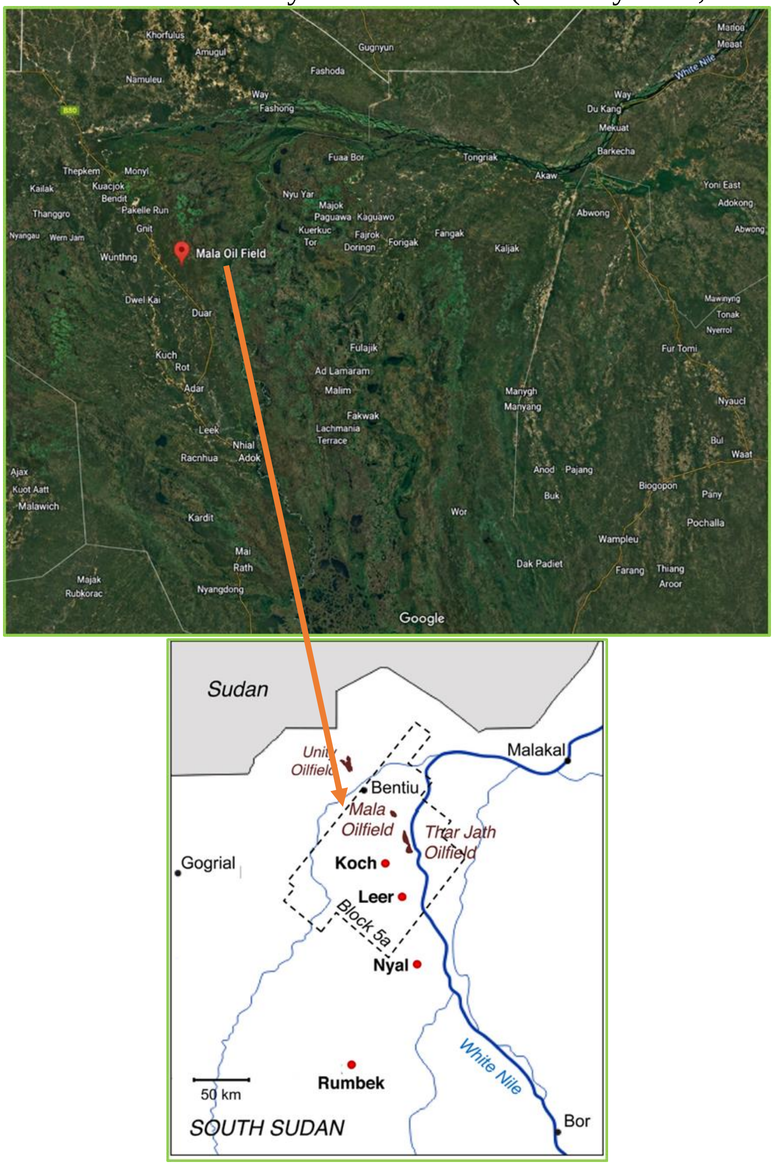

Figure 1: Map showing the location of Mala oil field (Pragst et al., 2017)

Materials and Methods

The dataset consists of existing petrophysical and reservoir modelling data, including Vp, Vs, acoustic impedance (AI), density (ρ), porosity ($\emptyset$), permeability (k), Lambda-Rho ($\lambda\rho$), Mu-Rho ($\mu\rho$), $Inz_S, Inz_P, In\rho$, density-neutron porosity, Flow Zone Indicator (FZI), Formation Micro Imager Tool (FMT) and Reservoir Quality Index (RQI). These data were screened, and integrated for simulation and interpretation purposes (Figure 2) for data consistency and to achieve the targets as stipulated and various cross-plots were derived as shown in the discussion.

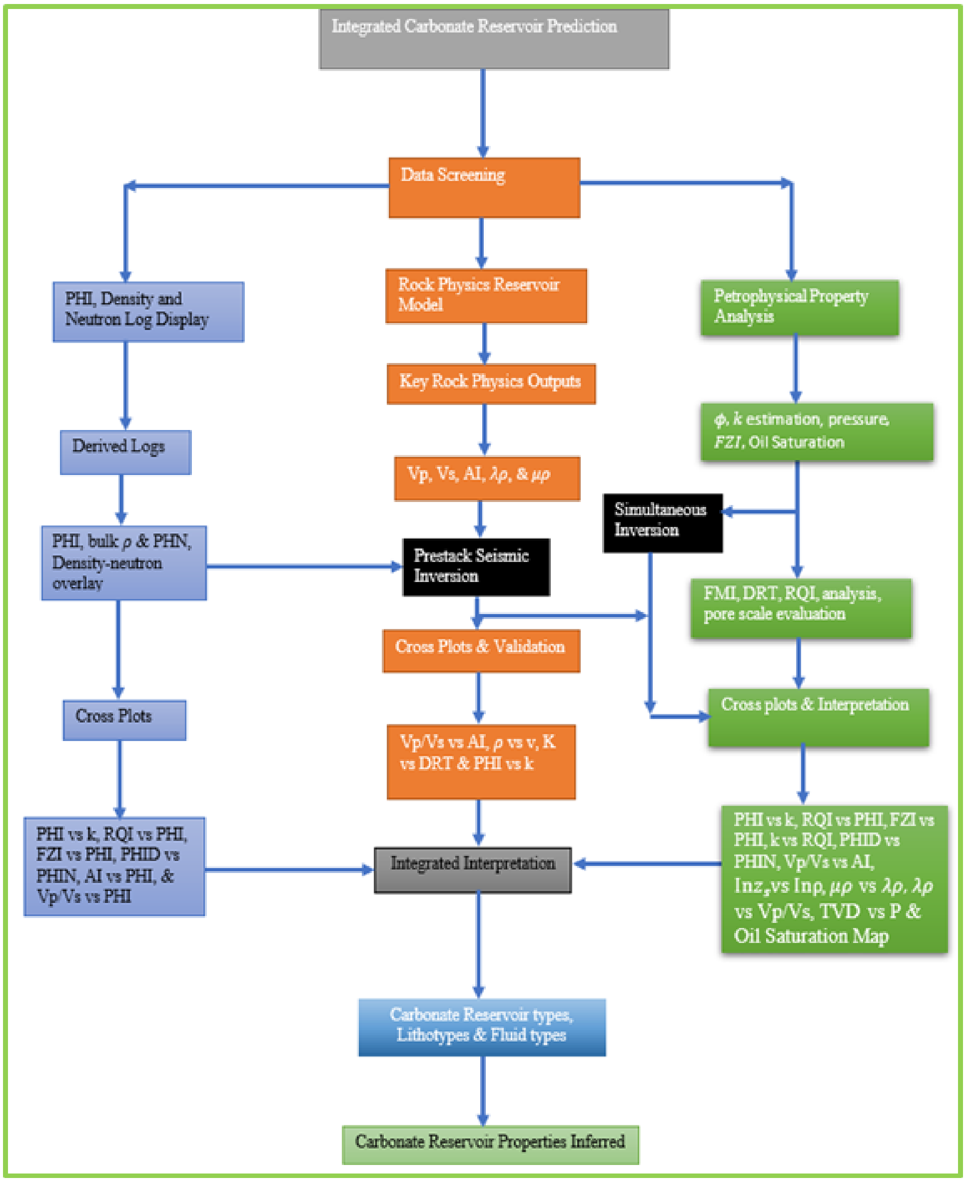

Figure 2: A summary of steps taken for reservoir properties prediction

Discussion and Conclusion
Discussion

The discussion is based on various cross-plots that are generated from the data including Vp, Vs, acoustic impedance (AI), density (ρ), porosity, permeability, Inz_S, Inz_P, velocity, Lambda-Rho $(\lambda\rho)$, Mu-Rho $(\mu\rho)$, density-neutron porosity, FZI, FMT and RQI. The prediction of carbonate reservoir properties is derived and discussed in accordance with the literature related to the cited cross-plots.

Predicting carbonate reservoir types based on the following cross-plots:

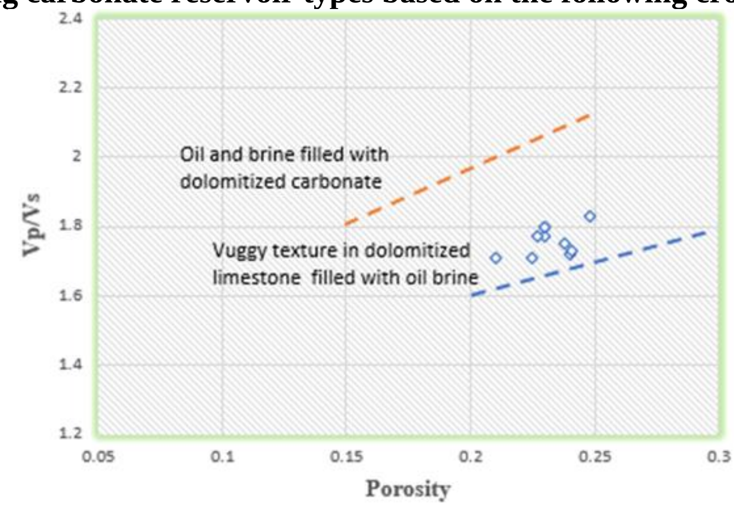

Figure 3: A cross-plot of Vp/Vs vs. Porosity, lines adapted from Asquith et al. (2004) & Rafavich et al. (1984), predicting dolomitized limestone reservoir characterized by chalky, moldic or vuggy texture, bearing brine oil with less amount of gas

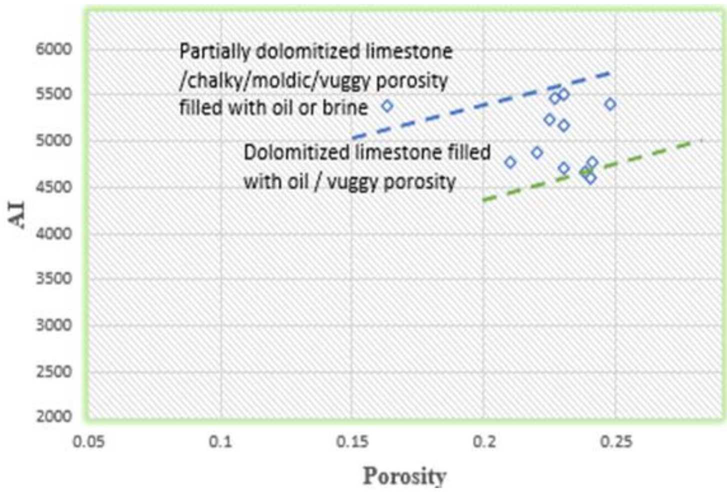

Figure 4: Acoustic Impedance (AI) vs. Porosity, a cross-plot adapted after Rafavich et al. (1984) indicate porous dolomitized carbonate limestone reservoir

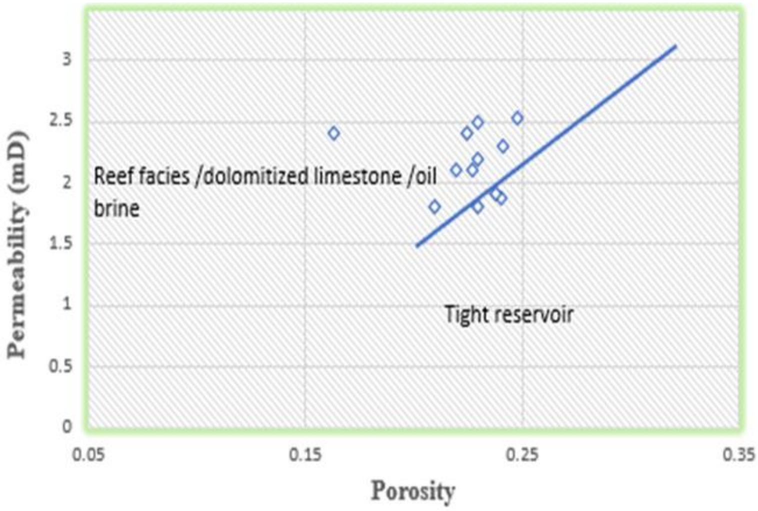

Figure 5: A modified cross-plot of Permeability vs. Porosity (Line drawn from Asquith et al., 2004; Tiab & Donaldson, 2012), showing reef reservoir bearing oil-brine prone, which characterized by coral and algae, and chalky mudstone and moldic sediments that are derived from dolomitized limestone reservoirs

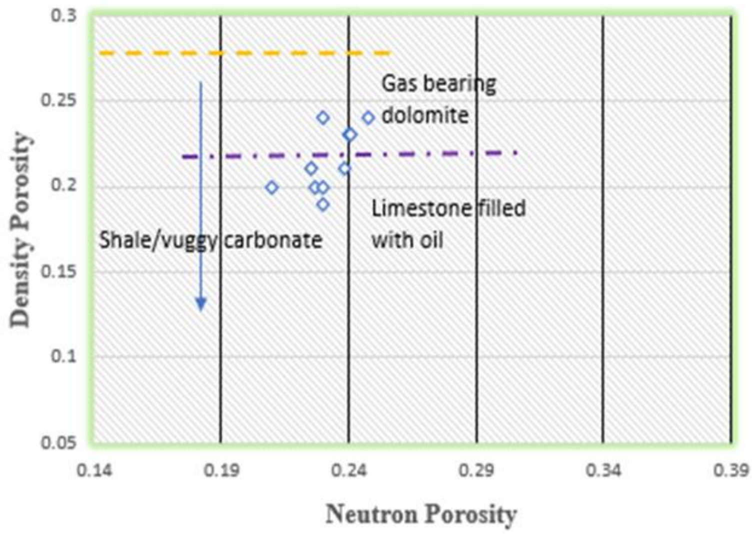

Figure 6: Density-Neutron Porosity cross-plot adapted from Asquith et al. (2004), which delineate porous dolomitized limestone reservoir bearing oil-gas zone filled with water

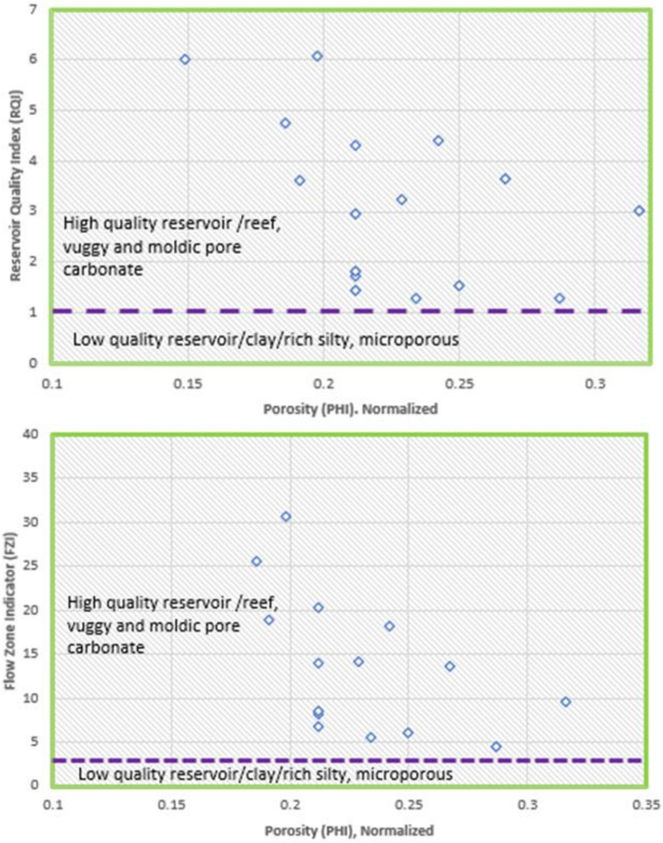

Figure 7: (above and below). A scattered plots extracted (A. H. Khan et al., 2019) & amaefule at al. (1993)suggest that reservoir has large vuggy, moldic pore throat, highly permeable reef carbonate reservoir

Lithotypes are determine from the listed cross-plots:

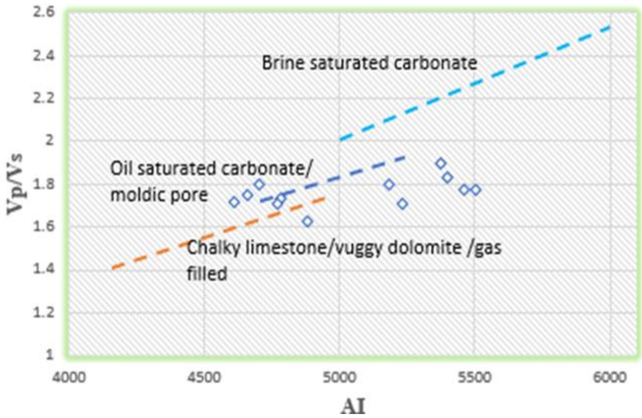

Figure 8: A modified cross-plot of Vp/Vs vs. AI (Li et al., 2018), illustrates chalky, vuggy dolomitized limestone reservoir as oil-gas prone indicating reservoir is hydrocarbon charged

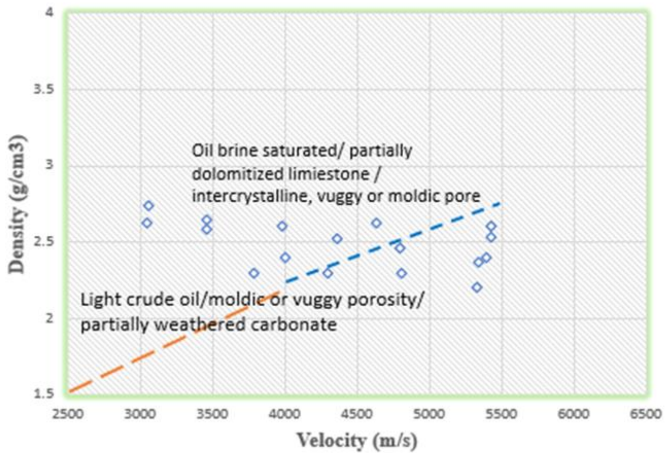

Figure 9: A cross-plot of Density vs. Velocity, modified after Weger et al. (2009), show dolomite facies dominated by condensed kerogen rich hydrocarbon (light), dominated by vuggy or karstic porosity

As stipulated from Figure 5 (Permeability vs. Porosity) above, shows chalky, mudstone sediment characterized by moldic porosity that are derived from dolomitized limestone.

Fluid Content is delineated from these cross-plots:

- From figure 5 (Permeability vs. Porosity) above, delineate the reservoir as bearing oil-brine prone.
- From figure 6 (Density vs. Neutron Porosity) above, it indicates the reservoir as oil-gas bearing zones filled with water.
- From figure 8 (Vp/Vs vs. AI) above, delineate the reservoir as oil-gas prone filled with saturated water.

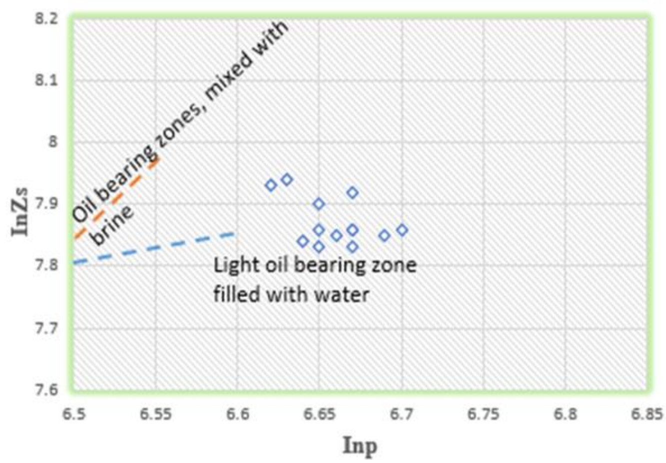

Figure 10: A scattered plot of $InZs$ vs. $In\rho$ (Lines drawn from Prayoga & Winardhi, 2022), show that the reservoir is oil prone filled with water

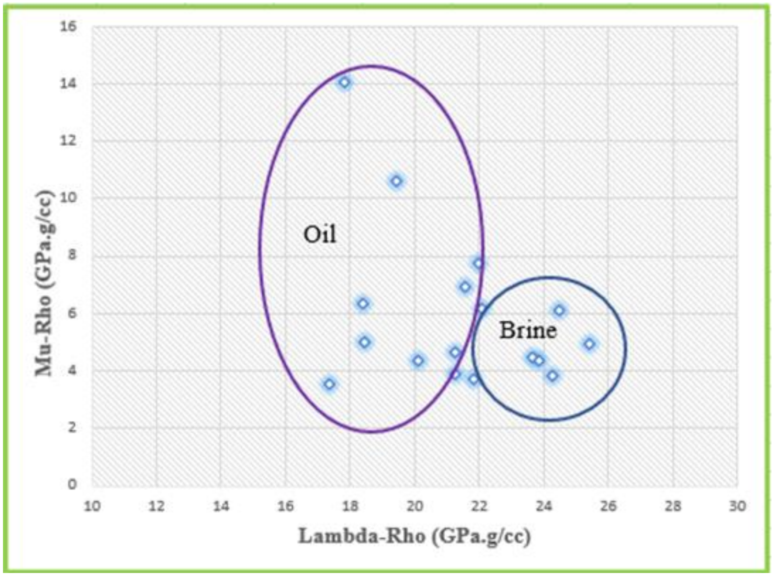

Figure 11: A scattered plot of Mu-Rho vs. Lamba-Rho ((K. I. et al., 2017), show that the reservoir is oil prone filled with brine

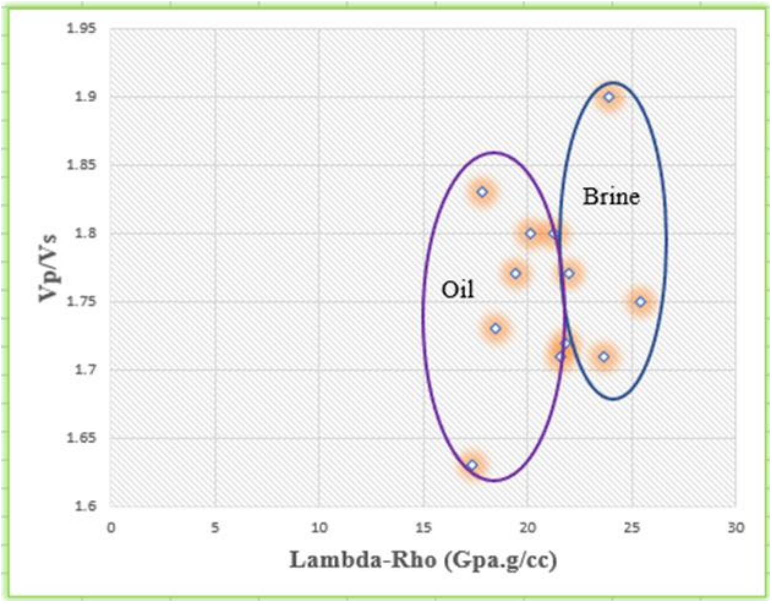

Figure 12: A scattered plot of Vp/Vs vs. Lamba-Rho (Adeoti et al., 2018) and (K. I. et al., 2017), show that the reservoir is oil prone filled with brine

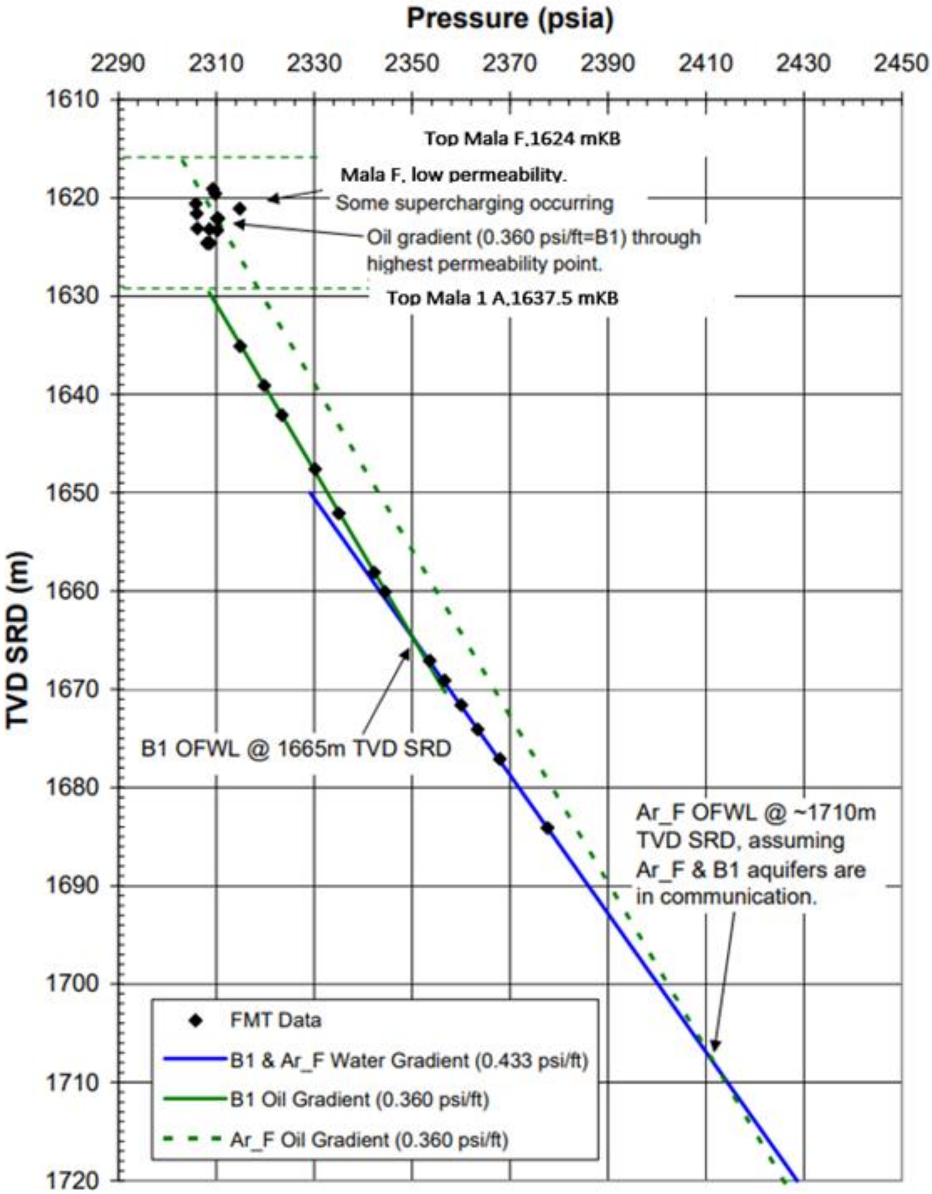

Figure 13: A simulation Pressure Profile (psia) against True Vertical Depth (m). This illustration suggest that the reservoir has both water and hydrocarbon (Wang et al., 2025)

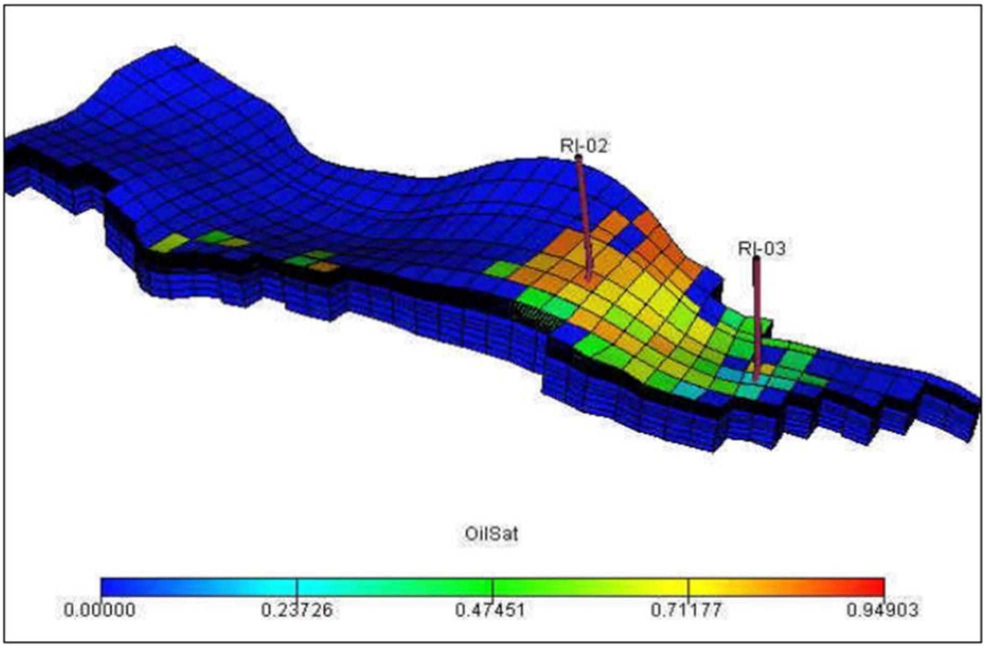

Figure 14: Oil Saturation Distribution Map, Dark blue areas shows very low oil saturation, light blue to green zones represent moderate oil saturation and yellow to red zone indicate high oil saturation

Conclusion

The integrated carbonate reservoir prediction model is based on various cross-plots and analysis illustrated in the discussion above, the selected reservoirs of Mala Oil Field exhibit good quality, characterized by moderate porosity and partially weathered dolomitized limestone lithologies, which consists of mudstone with chalky facies, moldic, vuggy, or karstic porosity, indicative of diagenetically altered, coral, alginite, and dolomitized limestone reefal carbonate reservoirs that exhibit condensed kerogen rich hydrocarbon. The petrophysical parameters suggest water and oil-gas bearing zones, dominated by moldic, vuggy or karstic porosity and secondary dissolution features.

Acknowledgements

I extend my deepest appreciation to School of Petroleum and Minerals (UoJ) and its dedicated staff for their invaluable support in facilitating the publication of this manuscript. I am especially thankful to my wife, Mary Nyang, and my children, Agwang Deng, Apul Deng, Atem Deng, for their constant encouragement, patience and understanding throughout the preparation of this manuscript.

Conflict of Interest: The authors reported no conflict of interest.

Data Availability: All data are included in the content of the paper.

Funding Statement: The author did not obtain any funding for this research.

References:

1. A. H. Khan, M. F., Abid, M. F., Fareed, A., Javed, Z., Khan, M. N., & Hashmi, S. (2019). Petrophysical Modelling of Structure-Cum-Stratigraphic Play for Improved Reservoir Potential, an Integrated Field Study of L. Goru Sands, Pakistan. SPE Annual Technical Conference and Exhibition, D021S032R003. https://doi.org/10.2118/196066-MS
2. Abuhagaza, A. A., El Sawy, M. Z., & Nabawy, B. S. (2021). Integrated petrophysical and petrographical studies for characterization of reservoirs: A case study of Muglad Basin, North Sudan. Environmental Earth Sciences, 80(5), 171. https://doi.org/10.1007/s12665-021-09489-7
3. Adeoti, L., Allo, O. J., Ayolabi, E. A., Akinmosin, A., Oladele, S., Oyeniran, T., & Ayuk, M. A. (2018). Reservoir fluid determination from angle stacked seismic volumes in 'Jay' field, Niger Delta, Nigeria. Journal of Applied Sciences and Environmental Management, 22(4), 453. https://doi.org/10.4314/jasem.v22i4.2
4. Alvarez, P., & Gebus, B. (2011, May 23). Mapping Porosity in a Carbonate Reservoir Using Seismic Inversion and Integration of the Result into a Geocelullar Model. 73rd EAGE Conference and Exhibition incorporating SPE EUROPEC 2011. https://doi.org/10.3997/2214-4609.20149557
5. Asquith, G., Krygowski, D., Henderson, S., & Hurley, N. (Eds.). (2004). Basic well log analysis (Second Edition). American Association of Petroleum Geologists. https://doi.org/10.1306/Mth16823
6. Avseth, P. (2010). Explorational Rock Physics – The Link Between Geological Processes and Geophysical Observables. In K. Bjorlykke, Petroleum Geoscience (pp. 403–426). Springer Berlin Heidelberg. https://doi.org/10.1007/978-3-642-02332-3_18
7. El Sawy, M. Z., Abuhagaza, A. A., Nabawy, B. S., & Lashin, A. (2020). Rock typing and hydraulic flow units as a successful tool for reservoir characterization of Bentiu-Abu Gabra sequence, Muglad basin, southwest Sudan. Journal of African Earth Sciences, 171, 103961. https://doi.org/10.1016/j.jafrearsci.2020.103961

8. Howarth, V., & Alves, T. M. (2016). Fluid flow through carbonate platforms as evidence for deep-seated reservoirs in Northwest Australia. Marine Geology, 380, 17–43. https://doi.org/10.1016/j.margeo.2016.06.011
9. K. I., U., I. O, A., & E. B., U. (2017). Derived Rock Attributes Analysis for Enhanced Reservoir Fluid and Lithology Discrimination. IOSR Journal of Applied Geology and Geophysics, 5(02), 95–105. https://doi.org/10.9790/0990-05020195105
10. Li, Y., Kang, Z., Xue, Z., & Zheng, S. (2018). Theories and practices of carbonate reservoirs development in China. Petroleum Exploration and Development, 45(4), 712–722. https://doi.org/10.1016/S1876-3804(18)30074-0
11. Mohammed, M. A. G. (2023). PETROLEUM GEOLOGY OF MUGLAD BASIN, SUDAN. 10(7).
12. Pragst, F., Stieglitz, K., Runge, H., Runow, K.-D., Quig, D., Osborne, R., Runge, C., & Ariki, J. (2017). High concentrations of lead and barium in hair of the rural population caused by water pollution in the Thar Jath oilfields in South Sudan. Forensic Science International, 274, 99–106. https://doi.org/10.1016/j.forsciint.2016.12.022
13. Prayoga, B. A., & Winardhi, S. (2022). Identification of Carbonate Reservoir Prospective Zones Using Rock Physics Approach and Extended Elastic Impedance (EEI) in "BAP" Field, South Sumatera Basin. IOP Conference Series: Earth and Environmental Science, 1031(1), 012019. https://doi.org/10.1088/1755-1315/1031/1/012019
14. Rafavich, F., Kendall, C. H. St. C., & Todd, T. P. (1984). The relationship between acoustic properties and the petrographic character of carbonate rocks. GEOPHYSICS, 49(10), 1622–1636. https://doi.org/10.1190/1.1441570
15. Reza, M. F., Rosid, M. S., & Haidar, M. W. (2019). Carbonate reservoir characterization using simultaneous inversion in field "X." 020023. https://doi.org/10.1063/1.5132450
16. Tiab, D., & Donaldson, E. C. (Eds.). (2012). Petrophysics: Theory and practice of measuring reservoir rock and fluid transport poperties (3rd ed). Gulf Professional Pub./Elsevier.
17. Wang, M., Zhang, X., Ji, Y., Liu, Y., Wang, T., Xing, Z., & Han, G. (2025). Research on Optimization Method of Operating Parameters for Electric Submersible Pumps Based on Multiphase Flow Fitting. 1–20.
18. Weger, R. J., Eberli, G. P., Baechle, G. T., Massaferro, J. L., & Sun, Y.-F. (2009). Quantification of pore structure and its effect on sonic velocity and permeability in carbonates. AAPG Bulletin, 93(10), 1297–1317. https://doi.org/10.1306/05270909001